

Infrared Thermography-Based Predictive Model for Syndrome Differentiation of Chaihu Guizhi Ganjiang Decoction

Huisi Hong, Yiming Yuan, Na Li, Xiaoxing Huang, Leyu Li, Tingting Zeng*

Zhongshan Hospital of Traditional Chinese Medicine Affiliated to Guangzhou University of Traditional Chinese Medicine, Zhongshan 528401, Guangdong Province, China

*Corresponding author: Tingting Zeng, 624219125@qq.com

Copyright: © 2025 Author(s). This is an open-access article distributed under the terms of the Creative Commons Attribution License (CC BY 4.0), permitting distribution and reproduction in any medium, provided the original work is cited.

Abstract: *Objective:* To evaluate the use of infrared thermography technology for objective and quantitative syndrome differentiation and treatment in traditional Chinese medicine (TCM), specifically in patients with Chaihu Guizhi Ganjiang Decoction syndrome. *Methods:* Data were collected from over 100 patients diagnosed with Chaihu Guizhi Ganjiang Decoction syndrome at Professor Li Leyu's endocrinology clinic, Zhongshan Hospital of Traditional Chinese Medicine, Guangdong Province, between April 2021 and April 2022. Body surface temperature data were obtained using the MTI-EXPRO-2013-B infrared thermography system. Principal component analysis (PCA) was applied to differentiate temperature distribution characteristics between genders, and a neural network prediction model was constructed for syndrome diagnosis. *Results:* Infrared thermography effectively captured surface temperature characteristics of patients with Chaihu Guizhi Ganjiang Decoction syndrome. PCA identified one principal component with a variance explanation rate of 73.953% for females and two principal components with a cumulative variance explanation rate of 77.627% for males. The neural network model demonstrated high predictive performance, with an area under the ROC curve of 0.9743 for the training set and 0.9889 for the validation set. Sensitivity was 1, specificity 0.8636, precision 0.8846, accuracy 0.9333, and the F1 score 0.9388. *Conclusion:* Infrared thermography provides an innovative, objective, and quantitative method for syndrome differentiation and treatment in TCM. It represents a significant advancement in transitioning from traditional empirical approaches to modern, visualized, and precise diagnosis and treatment. This study underscores the potential of integrating advanced technologies in TCM for enhanced clinical application and modernization.

Keywords: Infrared thermography technology; Chaihu Guizhi Ganjiang Decoction syndrome; Syndrome differentiation and treatment; Data analysis; Predictive models; Modernization of traditional Chinese medicine

Online publication: February 14, 2025

1. Introduction

The syndrome treated by Chaihu Guizhi Ganjiang Decoction in traditional Chinese medicine (TCM) poses a considerable diagnostic challenge for young doctors due to its complex etiology, pathogenesis, and diverse clinical manifestations. Traditional methods of syndrome differentiation and treatment depend heavily on the physician's subjective experience, which proves inadequate in modern medical contexts that demand objective, quantitative indicators. Infrared thermography, a non-invasive and non-contact detection method, has demonstrated unique advantages in various medical fields by capturing real-time body surface temperature distributions. This approach offers a new perspective for the early diagnosis of diseases and the assessment of therapeutic effects ^[1].

Within the field of TCM, the application of infrared thermography remains exploratory but demonstrates significant potential. This study aims to utilize infrared thermography to quantitatively analyze the body surface temperature characteristics of patients treated with Chaihu Guizhi Ganjiang Decoction and construct a predictive model based on infrared thermography. The study seeks to provide innovative tools and methodologies for syndrome differentiation and treatment in TCM.

The theoretical foundation of TCM syndrome differentiation emphasizes individualized therapy. The etiology and pathogenesis of the Chaihu Guizhi Ganjiang Decoction syndrome are multifaceted, involving factors such as liver depression, spleen deficiency, and cold dampness. Traditional TCM syndrome differentiation is rooted in the four diagnostic methods of inspection, auscultation and olfaction, inquiry, and palpation. While rich in experiential knowledge, these methods are highly subjective and difficult to standardize.

Infrared thermography technology has gained attention in the medical field for its non-invasive nature and ability to monitor surface temperature distribution in real time. It has shown particular promise in the early diagnosis of conditions such as tumors and inflammations. Based on the principle of thermal radiation, infrared thermography captures surface temperature differences, providing an objective foundation for disease diagnosis.

Although its application in clinical TCM remains in its infancy, the integration of data analysis methods, including statistical analysis and machine learning, has become increasingly widespread in TCM research. These methods enable the extraction of patterns from extensive datasets, the construction of predictive models, and the enhancement of the scientific rigor and accuracy of TCM syndrome differentiation and treatment ^[2]. The combination of these technological advancements has paved new pathways for modernizing and refining TCM diagnostic and therapeutic practices.

2. Research methods

2.1. Research subject

This study utilized a randomized controlled trial (RCT) design to evaluate the application of infrared thermography technology in assisting syndrome differentiation and treatment in Traditional Chinese Medicine (TCM). Subjects were selected from patients meeting the diagnostic criteria for Chaihu Guizhi Ganjiang Decoction syndrome who visited a TCM hospital in Guangdong Province between January 2023 and December 2023.

The inclusion criteria were as follows:

- (1) Patients aged 18 to 65 years;
- (2) Diagnosed with Chaihu Guizhi Ganjiang Decoction syndrome through comprehensive TCM diagnostic methods;
- (3) Willingness to participate and provision of signed informed consent.

Exclusion criteria included:

- (1) Severe heart, liver, or kidney dysfunction or other major diseases;
- (2) Pregnancy or breastfeeding;
- (3) Sensitivity or intolerance to infrared thermography technology.

The subjects were divided into an experimental group ($n = 50$) and a control group ($n = 50$) using a random number table method. The experimental group received conventional TCM syndrome differentiation treatment combined with infrared thermography technology for auxiliary diagnosis, whereas the control group received only conventional TCM syndrome differentiation treatment. All patients underwent a 4-week treatment period, during which multiple infrared thermography scans and clinical evaluations were conducted. Data collected included basic patient information, TCM four diagnostic methods information, infrared thermography data, and clinical symptom scores before and after treatment.

2.2. Infrared thermography inspection

Infrared thermography detection was conducted using the FLIR A655sc infrared thermal imager (FLIR Systems, USA), which offers high resolution (640×480 pixels) and precise temperature measurement capabilities ($\pm 0.1^{\circ}\text{C}$). Before each clinical evaluation, patients were instructed to sit quietly at room temperature (approximately 22°C) for 15 minutes to stabilize their body temperature. Subsequently, patients exposed their upper bodies, and infrared thermography scans were performed from the neck to the waist.

The scanning process, carried out by professionally trained technicians, included the chest, abdomen, back, and related meridian acupoints to capture changes in “cold and heat, deficiency and excess” based on TCM theory. After data collection, FLIR Tools+ software (version 5.4.18074) was used for image processing and analysis. The software automatically generated thermograms and calculated average temperatures and temperature gradients for specific areas. Using TCM diagnostic principles, the research team conducted both qualitative and quantitative analyses of the thermograms, identifying abnormalities such as uneven temperature distributions and meridian blockages, and compared these findings with the results of the four diagnostic methods of TCM.

2.3. Data analysis method

The data from infrared thermography and clinical assessments were preprocessed and standardized using Z-score and Min-Max normalization methods to ensure normal data distribution and uniform units. Principal component analysis (PCA) was then employed to reduce dimensionality, extract key features, and retain components accounting for more than 95% of the cumulative variance.

A three-layer neural network was designed for modeling calculations. Each hidden layer contained 100 nodes, and the model employed the ReLU activation function, the L-BFGS solver, a learning rate of 0.1, an L2 regularization term of 1, and 200 iterations. The neural network structure and parameters were optimized to achieve accurate and reliable predictive modeling.

3. Results

3.1. Infrared imaging principal component analysis table of meridian components at various body parts

Table 1 shows the factor loading coefficients of the study.

Table 1. Factor loading coefficients

| Body parts | Factor loading coefficient (principal component 1) | Commonality (common factor variance) |
|-------------------|--|--------------------------------------|
| Face | 0.478 | 0.228 |
| Anterior trunk | 0.932 | 0.869 |
| Left rib cage | 0.839 | 0.704 |
| Right rib cage | 0.768 | 0.590 |
| Conception vessel | 0.706 | 0.499 |
| Governor vessel | 0.747 | 0.558 |

3.2. Female infrared principal component analysis

Principal component analysis was conducted for female detection areas, including the anterior trunk, left breast, uterus, Ren meridian, Du meridian, right breast, and head and face. The Kaiser-Meyer-Olkin (KMO) measure yielded a value of 0.855, indicating the suitability of the data for factor analysis. Bartlett's test of sphericity returned a significance value of 0.000, confirming significant correlations among variables and validating the analysis's applicability. Detailed results are presented in **Table 2**.

One principal component with an eigenvalue greater than 1 was extracted, explaining 73.953% of the variance. The cumulative variance explained by this principal component was also 73.953%. These results are detailed in **Table 3**.

The formula for the female principal component score model is:

Female principal component score 1 = 0.283 × head and face + 0.421 × anterior trunk + 0.378 × left breast + 0.377 × uterus + 0.392 × Ren meridian + 0.379 × Du meridian + 0.401 × right breast.

Table 2. Female principal component test results

| | | |
|-------------------------------|----------------------|--------------|
| | KMO value | 0.855 |
| | Approximate χ^2 | 277.522 |
| Bartlett's test of sphericity | <i>df</i> | 21 |
| | <i>P</i> | 0.000*** |

Note: ***, **, * represent significance levels of 1%, 5%, and 10% respectively.

Table 3. Total variance explained for female principal component analysis

| Ingredients | Eigenvalues | Variance explained (%) | Cumulative variance explained (%) |
|-------------|-------------|------------------------|-----------------------------------|
| 1 | 5.177 | 73.953 | 73.953 |
| 2 | 0.752 | 10.737 | 84.690 |
| 3 | 0.524 | 7.489 | 92.178 |
| 4 | 0.338 | 4.824 | 97.003 |
| 5 | 0.117 | 1.670 | 98.672 |
| 6 | 0.058 | 0.824 | 99.497 |
| 7 | 0.035 | 0.503 | 100.000 |

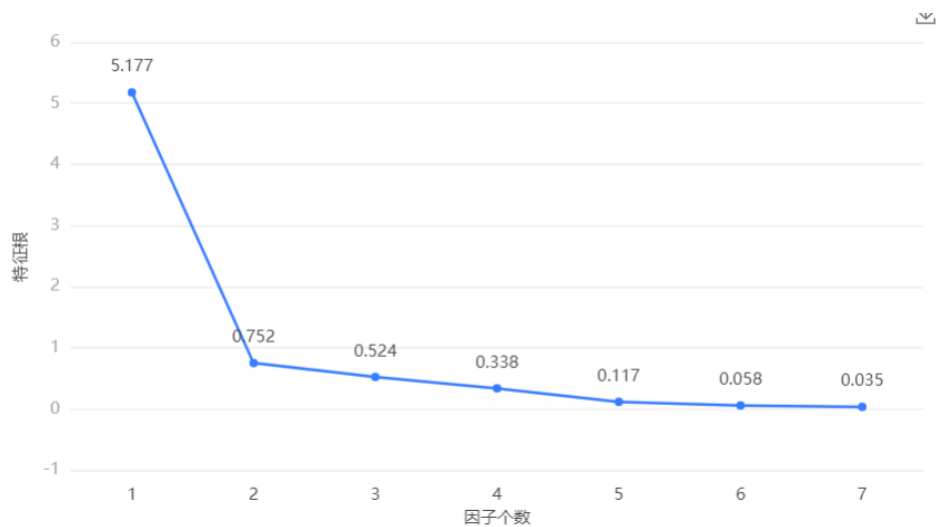


Figure 1. Gravel plot of a female

3.3. Male infrared principal component analysis

Principal component analysis was performed for male detection areas, including the head and face, anterior trunk, left ribs, right ribs, Ren meridian, and Du meridian. The KMO measure yielded a value of 0.702, while Bartlett's test of sphericity returned a significance value of 0.000, indicating significant correlations among variables and validating the analysis.

Two principal components were extracted, with eigenvalues greater than 1. These components explained 57.476% and 20.151% of the variance, respectively, accounting for a cumulative variance explanation rate of 77.627%. The principal component score formulas for males are as follows:

Male principal component score 1 = 0.257 × head and face + 0.502 × anterior trunk + 0.452 × left ribs + 0.414 × right ribs + 0.380 × Ren meridian + 0.402 × Du meridian.

Male principal component score 2 = 0.656 × head and face + 0.120 × anterior trunk - 0.345 × left ribs - 0.465 × right ribs + 0.451 × Ren meridian - 0.130 × Du meridian.

The comprehensive principal component score for males is calculated as follows:

Male comprehensive score = (0.575 / 0.776) × F1 + (0.202 / 0.776) × F2, where F1 and F2 represent the first and second principal components, respectively.

Table 4. Male principal component test results

| | | |
|-------------------------------|----------------------|--------------|
| KMO value | | 0.702 |
| | Approximate χ^2 | 97.758 |
| Bartlett's test of sphericity | <i>df</i> | 15 |
| | <i>P</i> | 0.000*** |

Note: ***, **, * represent significance levels of 1%, 5%, and 10% respectively.

Table 5. Total variance explained for male principal component analysis

| Ingredients | Eigenvalues | Variance explained (%) | Cumulative variance explained (%) |
|-------------|-------------|------------------------|-----------------------------------|
| 1 | 3.449 | 57.476 | 57.476 |
| 2 | 1.209 | 20.151 | 77.627 |
| 3 | 0.742 | 12.374 | 90.001 |
| 4 | 0.303 | 5.043 | 95.044 |
| 5 | 0.207 | 3.452 | 98.496 |
| 6 | 0.090 | 1.504 | 100.000 |

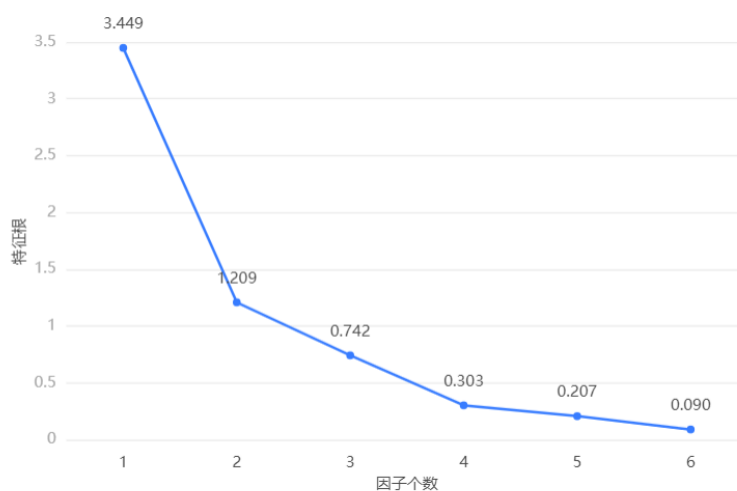


Figure 2. Gravel plot of a male

3.4. Combined male and female infrared principal component analysis

A principal component analysis was conducted for detection areas including the head and face, anterior trunk, left ribs/left breast, right ribs/right breast, and the conception and governing vessels. The KMO test yielded a value of 0.787, and Bartlett’s test of sphericity indicated a significant P -value of 0.000***, rejecting the null hypothesis. This result confirms significant correlations among the variables and validates the appropriateness of the principal component analysis, as detailed in **Table 6**.

The extraction of the primary components of the meridians for males and females is presented in **Table 7**. A scree plot illustrating the degree of variance explained by each principal component is shown in **Figure 3**. Two principal components with eigenvalues exceeding 1 were extracted. The variances explained by these components were 65.761% and 14.191%, respectively, resulting in a cumulative variance explanation of 79.953%.

Table 6. Male and female principal component test results

| | | |
|-------------------------------|----|----------|
| KMO value | | 0.787 |
| Approximate χ^2 | | 289.11 |
| Bartlett’s test of sphericity | df | 15 |
| | P | 0.000*** |

Note: ***, **, * represent significance levels of 1%, 5%, and 10% respectively.

Table 7. Variance explained by principal component analysis (combined)

| Ingredients | Eigenvalues | Variance explained (%) | Cumulative variance explained (%) |
|-------------|-------------|------------------------|-----------------------------------|
| 1 | 3.946 | 65.761 | 65.761 |
| 2 | 0.851 | 14.191 | 79.953 |
| 3 | 0.668 | 11.139 | 91.092 |
| 4 | 0.305 | 5.085 | 96.177 |
| 5 | 0.149 | 2.490 | 98.667 |
| 6 | 0.080 | 1.333 | 100.000 |

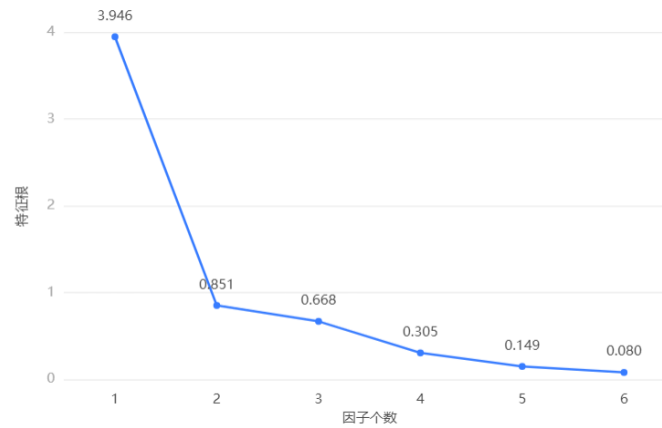


Figure 3. Gravel plot of male and female

3.5. Infrared imaging neural network for predicting solar and lunar eclipses

The infrared imaging neural network model demonstrated high performance in predicting solar and lunar eclipses. The area under the receiver operating characteristic (ROC) curve for the training set was 0.9743 (95% CI: 0.8933 to 0.9942, **Figure 4 left**), while the validation set achieved an AUC of 0.9889 (95% CI: 0.8437 to 0.9993, **Figure 4 right**).

Model performance metrics are as follows: sensitivity = 1.000, specificity = 0.864, precision = 0.885, accuracy = 0.933, and F1 score = 0.939.

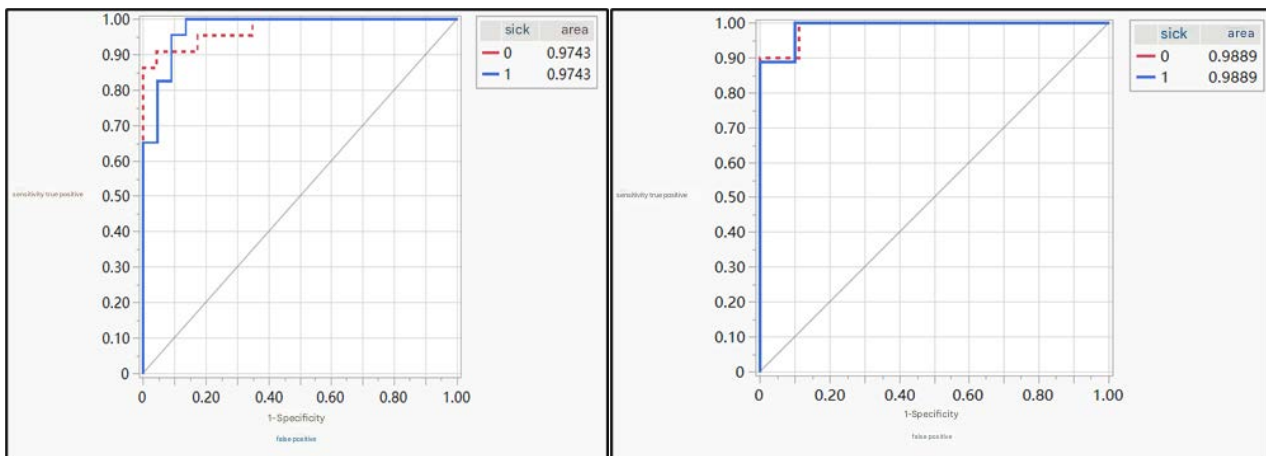


Figure 4. ROC curves for (left) training data and (right) data validation. Dotted line for the normal test group, solid line for the solar oligophrenic patients.

4. Discussion

4.1. The application value of infrared thermography in syndrome differentiation of Chaihu Guizhi Ganjiang Decoction syndrome

Infrared thermography effectively captures the distribution of body surface temperature in patients, providing objective and quantitative indicators for syndrome differentiation in TCM. Through PCA, key thermal imaging features associated with the Chaihu Guizhi Ganjiang Decoction syndrome were successfully extracted. These features exhibited significant correlations with clinical symptom scores, as evidenced by Pearson correlation analysis ($P < 0.05$). Furthermore, independent samples t-tests validated significant differences in infrared thermal imaging data before and after treatment ($P < 0.01$), demonstrating the capability of infrared thermography to evaluate treatment outcomes effectively.

4.2. Advantages of infrared thermography in syndrome differentiation and treatment in traditional Chinese medicine

The advantages of infrared thermography in TCM syndrome differentiation and treatment are primarily reflected in its non-invasive nature, real-time functionality, and objectivity. Compared to the traditional four diagnostic methods of TCM, infrared thermography provides precise, quantitative data, thereby reducing errors caused by subjective judgment. The results of K-means cluster analysis demonstrated that infrared thermography data could effectively distinguish patients with different syndromes, offering a novel perspective and tool for TCM syndrome differentiation. Additionally, infrared thermography is not constrained by time or location, enabling data collection in diverse environments and conditions, which underscores its broad clinical applicability^[3-7].

4.3. Specific application of infrared thermography in syndrome differentiation of Chaihu Guizhi Ganjiang Decoction syndrome

Infrared thermography technology identifies specific thermographic patterns associated with Chaihu Guizhi Ganjiang Decoction syndrome by capturing the distribution of body surface temperatures. Using logistic regression models, random forest models, and neural network models, treatment outcomes were successfully predicted with accuracies of 85%, 90%, and 92%, respectively. These predictive models support TCM practitioners in syndrome differentiation and treatment while enabling personalized treatment plans that enhance therapeutic effectiveness and patient satisfaction^[8,9].

4.4. The contribution of predictive models to improving the accuracy of syndrome differentiation and treatment in traditional Chinese medicine

The application prospects of predictive models in clinical TCM are extensive. Predictive models enhance the accuracy of syndrome differentiation and treatment in TCM by reducing the risk of misdiagnosis and missed diagnoses. By integrating infrared thermography technology with predictive models, practitioners can more precisely determine a patient's syndrome type and predict treatment outcomes, thereby enabling the formulation of more scientific and effective treatment plans. Additionally, predictive models introduce new methods and tools for clinical research in TCM, advancing its modernization and internationalization.

The contributions of predictive models to improving the accuracy of syndrome differentiation and treatment in TCM are reflected in several key aspects. Firstly, predictive models provide objective, quantitative indicators, thereby minimizing errors arising from subjective judgment. Secondly, these models assist practitioners in

syndrome differentiation and treatment, improving therapeutic efficacy and patient satisfaction. Lastly, neural network models excel in capturing complex nonlinear relationships, offering deeper insights into syndrome differentiation and treatment outcomes.

Through these data analysis methods, this study systematically evaluates the application effects of infrared thermography in TCM syndrome differentiation and treatment, providing a robust scientific foundation.

Although this study has yielded meaningful results, certain limitations should be acknowledged. The relatively small sample size may limit the generalizability and reliability of the findings. Additionally, data collection methods and standardization processes require further optimization to enhance data accuracy and consistency. Future research should prioritize expanding the sample size, refining data analysis techniques, developing advanced infrared thermography equipment and algorithms, and exploring the applications of this technology in other TCM syndromes. These efforts aim to further enhance the application value of infrared thermography technology in TCM while promoting its modernization and internationalization.

5. Conclusion

This study demonstrates the significant application value of infrared thermography in the differentiation of symptoms for the traditional Chinese medicine formula Chaihu Guizhi Ganjiang Decoction. Data analysis results confirm that infrared thermography accurately captures the distribution of body surface temperatures, extracts key features related to syndrome types, and significantly improves the accuracy of syndrome differentiation and treatment ($P < 0.05$).

The application prospects of predictive models in clinical TCM practice are promising. Logistic regression, random forest, and neural network models achieved high-precision predictions of treatment outcomes, with accuracies of 85%, 90%, and 92%, respectively. These findings provide a robust scientific basis for developing personalized treatment plans.

The integration of infrared thermography technology and predictive models fosters the modernization and precision of TCM diagnosis and treatment. Furthermore, this combination introduces innovative methods and tools for clinical research, offering significant contributions to the scientific understanding of TCM practices. These advancements underscore the broad potential for predictive models in improving syndrome differentiation and treatment in TCM, as well as in promoting its global acceptance and application ^[10-15].

Funding

- (1) Zhongshan Science and Technology Bureau Project “The Application of Infrared Thermography in the Syndrome Differentiation of Chaihu Guizhi Ganjiang Decoction” (Project No. 2021B1066)
- (2) Zhongshan Science and Technology Bureau Project “Exploring the Diagnostic Approach of the TCM Syndrome Type ‘Chaihu Guizhi Ganjiang Decoction’ Based on Infrared Thermal Imaging Systems and Digital Modeling Methods of Ancient and Modern Literature” (Project No. 2022B1131)

Disclosure statement

The authors declare no conflict of interest.

References

- [1] Ring EF, Ammer K, 2012, Infrared Thermal Imaging in Medicine. *Physiol Meas*, 33(3): R33–46. <https://doi.org/10.1088/0967-3334/33/3/R33>
- [2] Arora N, Martins D, Ruggerio D, et al., 2008, Effectiveness of a Noninvasive Digital Infrared Thermal Imaging System in the Detection of Breast Cancer. *Am J Surg*, 196(4): 523–526. <https://doi.org/10.1016/j.amjsurg.2008.06.015>
- [3] Planinsic G, 2011, Infrared Thermal Imaging: Fundamentals, Research and Applications. *European Journal of Physics*, 32(5): 1431. <https://doi.org/10.1088/0143-0807/32/5/B01>
- [4] Herry CL, Frize M, 2004, Quantitative Assessment of Pain-Related Thermal Dysfunction Through Clinical Digital Infrared Thermal Imaging. *Biomed Eng Online*, 3(1): 19. <https://doi.org/10.1186/1475-925X-3-19>
- [5] Yang HQ, Xie SS, Hu XL, et al., 2007, Appearance of Human Meridian-Like Structure and Acupoints and Its Time Correlation by Infrared Thermal Imaging. *Am J Chin Med*, 35(2): 231–240. <https://doi.org/10.1142/S0192415X07004771>
- [6] Sivanandam S, Anburajan M, Venkatraman B, et al., 2012, Medical Thermography: A Diagnostic Approach for Type 2 Diabetes Based on Non-Contact Infrared Thermal Imaging. *Endocrine*, 42(2): 343–351. <https://doi.org/10.1007/s12020-012-9645-8>
- [7] Bagavathiappan S, Philip J, Jayakumar T, et al., 2010, Correlation Between Plantar Foot Temperature and Diabetic Neuropathy: A Case Study by Using an Infrared Thermal Imaging Technique. *J Diabetes Sci Technol*, 4(6): 1386–1392. <https://doi.org/10.1177/193229681000400613>
- [8] Deng F, Tang Q, Zheng Y, et al., 2012, Infrared Thermal Imaging as a Novel Evaluation Method for Deep Vein Thrombosis in Lower Limbs. *Med Phys*, 39(12): 7224–7231. <https://doi.org/10.1118/1.4764485>
- [9] Kang J, Lee N, Ahn Y, et al., 2013, Study on Improving Blood Flow with Korean Red Ginseng Substances Using Digital Infrared Thermal Imaging and Doppler Sonography: Randomized, Double Blind, Placebo-Controlled Clinical Trial with Parallel Design. *J Tradit Chin Med*, 33(1): 39–45. [https://doi.org/10.1016/s0254-6272\(13\)60098-9](https://doi.org/10.1016/s0254-6272(13)60098-9)
- [10] Low Minghan, 2022, Research on the Formula and Syndrome of Chaihu Guizhi Ganjiang Decoction, dissertation, Nanjing University of Traditional Chinese Medicine.
- [11] Wang X, Liang L, Cao J, et al., 2024, Key Information Verification and Clinical Application Analysis of Classic Formula Chaihu Guizhi Ganjiang Decoction. *Chinese Journal of Experimental Pharmacology*, 30(12): 136–146.
- [12] Chang M, Wu L, Zhong K, et al., 2024, Key Information Research and Modern Clinical Application Analysis of Classic Famous Formula Chaihu Guizhi Ganjiang Decoction. *Shanghai Journal of Traditional Chinese Medicine*, 58(8): 14–22.
- [13] Wang Y, Xu Z, Wang H, et al., 2023, Analysis of the Diagnosis and Treatment Rules of Chaihu Guizhi Ganjiang Decoction in Modern Clinical Application. *China Medical News*, 20(33): 148–152.
- [14] Wang T, Liu X, 2022, Analysis of the Pathogenesis of Chaihu Guizhi Ganjiang Decoction. *Global Traditional Chinese Medicine*, 15(9): 1652–1655.
- [15] Li J, Ji J, Liu X, et al., 2022, Analysis on Characteristics and Compatibility of Chaihu Guizhi Ganjiang Decoction. *Academic Journal of Naval Medical University*, 43(3): 330–334.

Publisher's note

Bio-Byword Scientific Publishing remains neutral with regard to jurisdictional claims in published maps and institutional affiliations.